J Incl Phenom Macrocycl Chem (2012) 73:99–108
DOI 10.1007/s10847-011-0025-4

ORIGINAL ARTICLE

Host–guest complexation between 5-aminoisoquinoline and β-cyclodextrin and its effect on spectral and prototropic characteristics

Rajaram Rajamohan · Sundarrajulu Kothai Nayaki · Meenakshisundaram Swaminathan

Received: 15 October 2010 / Accepted: 26 July 2011 / Published online: 19 August 2011

Abstract The effects of the addition of β-cyclodextrin (β-CDx) on the absorption and emission properties of the 5-aminoisoquinoline (5AIQ) have been investigated in aqueous media. The formation of host–guest inclusion complex with 1:1 stoichiometry was revealed by absorption, steady state and time-resolved emission spectroscopy. The complex formation has also been confirmed by FT-IR spectra and SEM image analysis of the solid inclusion complex between 5AIQ and β-CDx. No significant change was observed in the ground and excited state p*K*a values in β-CDx medium. Based on photophysical and prototropic characteristics of 5AIQ in β-CDx, the structure of the 1:1 inclusion complex is proposed.

Keywords 5-Aminoisoquinoline-β-cyclodextrin-inclusion complex · Excited state acidity constant

Introduction

Cyclodextrins (CDx) are cyclic oligosaccharides consisting of six (α-CDx), seven (β-CDx) or eight (γ-CDx) units of α-D-glucose linked together by α-(1,4) bonds. They are shaped like truncated cones, with a smaller and larger rim opening at the primary hydroxyl and secondary hydroxyl faces of the cyclic sugar network, respectively [1–3]. These molecules are characterised by a hydrophobic cavity and a relatively hydrophilic periphery due to the hydroxyl groups of the receptor edges. Such features center on CDx the ability to form water soluble inclusion complexes with several organic and inorganic substrates [1–6]. A number of factors influence complexation. The "goodness of fit" between host and guest and the hydrophobic effect are probably the most important [7, 8]. Encapsulation and photochemical investigation in such organized assemblies is an extremely active area of research in the field of supramolecular chemistry for both fundamental studies and practical purposes [9–12].

Fluorescence spectroscopy is a powerful tool for the study of the reactivity of chemical and biological systems since it allows non-intrusive measurements of substances in low concentration under physiological conditions and it is also sensitive to the environment [13]. The chemical reactivity and the spectroscopic properties of the guest molecules are modified as a result of the inclusion [2, 3, 7, 8, 14]. In particular, ground and singlet excited state protolytic equilibria are influenced because of the variation of microenvironment experienced by the included guest [14, 15].

The effect of substituent in the spectral characteristics of N-heterocyclic molecule in the ground and excited state have been a topic of intensive experimental investigation for a long time. These type of molecules make inclusion complexes with different cyclic molecules such as cyclodextrins.

Compounds containing a fused quinazoline or isoquinoline ring belong to a broad class of compounds, which received a considerable attention over the past years due to their wide range of biological activities [16, 17] Some of aminoquinazoline derivatives were found to be inhibitors

R. Rajamohan
Department of Chemistry, SKP Institute of Technology, Tiruvannamalai 606 611, India

S. Kothai Nayaki
Chemistry Section, FEAT, Annamalai University, Annamalainagar, Chidambaram 608 002, India

M. Swaminathan (✉)
Department of Chemistry, Annamalai University, Annamalainagar, Chidambaram 608 002, India
e-mail: chemres50@gmail.com

of the tyrosine kinase [18, 19] or dihydrofolate reductase enzymes [20, 21] so they work as potent anticancer agents. They are also used to work out medicines against hypertension, malaria and to fight infections involving AIDS [22]. Some isoquinoline derivatives are known due to the central nervous- system activity which they show [23].

The excited state proton transfer (ESPT) of 2′-hydroxy-2-trans-styrylquinoline was studied in CDx by Shun-Li et al [24]. ESPT and dual emission of substituted benzothiazoles and benzimidazoles were investigated [25].

Our laboratory has been active for years in studying the acid–base properties of some amino and hydroxy substituted biphenyl compounds in aqueous medium [26–28]. Recently we have reported the spectral characteristics and ESPT of some amino substituted ethers and benzisothiazoles with β-cyclodextrin [29–31]. In this paper, we present the effects of complexation by β-CDx on the spectral and prototropic characteristics of 5AIQ.

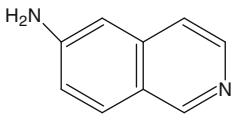

5AIQ

Experimental

Materials

5AIQ was obtained from Aldrich Co and purified by recrystallization from aqueous ethanol. β-CDx was purchased from S.D. fine chemicals and used as received. Triple distilled water was used for the preparation of experimental solutions. A modified Hammett acidity scale (H_0) [32] was employed for the solutions below pH 1.5 (using a H_2SO_4–H_2O mixture). The concentration of the experimental solution was 2.30×10^{-5} mol dm^{-3}. For estimation of binding constant, the temperature was kept at 303 K. To measure the fluorescence intensities for fluorimetric titration, the isosbestic wavelength was used for excitation.

Instruments

Absorption spectra were recorded with Shimadzu UPS 2001 spectrophotometer while fluorescence measurements were made using a Shimadzu RF-5301 PC spectrofluorometer. pH values in the range of 1–12 were measured using an ELICO LI-10T model pH meter. Fluorescence life-times were determined using a time-correlated picosecond photon counting spectrofluorometer (Tsunami, Spectraphysics, USA). FT-IR spectra were obtained from Avatar-330 FT-IR spectrophotometer using KBr pellet. The range of spectra was from 500 to 4000 cm^{-1}. Microscopic morphological structure measurements were performed with JEOL-JSM 5610LV scanning electron microscope (SEM). The bond distance calculations on the inclusion complex between 5AIQ and β-CDx were performed theoretically using a modified version of the computer programme Argus Lab, MOPAC/AM1.

Determination of binding constant of inclusion complex

Benesi–Hildebrand equation [33, 34] were used for the determination of binding constant of 1:1 complex from absorption (Eq. 1) and fluorescence (Eq. 2)

$$\frac{1}{\Delta A} = \frac{1}{\Delta\varepsilon[5\mathrm{AIQ}]_0} + \frac{1}{Ka[5\mathrm{AIQ}]_0\Delta\varepsilon[\beta\text{−}\mathrm{CDx}]_0} \quad (1)$$

where, ΔA is the difference between the absorbance of 5AIQ at 324.5 nm in the presence and absence of β-CDx. $\Delta\varepsilon$ is the difference between the molar extinction coefficients of 5AIQ and the inclusion complex. $[5\mathrm{AIQ}]_0$ and $[\beta\text{-CDx}]_0$ are the initial concentrations of guest and β-CDx, respectively and K is the binding constant. K was determined from slope of BH plot of $1/\Delta A$ Vs $1/\beta$-CDx.

$$\frac{1}{I - I0} = \frac{1}{I' - I_0} + \frac{1}{K(I' - I_0)(\beta - CDx)} \quad (2)$$

In the above equation, I_0 is the intensity of fluorescence of the 5AIQ without β-CDx, I is the intensity with a particular concentration of β-CDx, I′ is the intensity at the maximum concentration of β-CDx used and K is the binding constant. The binding constant K was calculated from the slope of Benesi-Hildebrand plot of $1/(I - I_0)$ vs. $1/\beta$-CDx

Calculation of ground state acidity constant

Absorption spectra of an acid and its conjugate base were different enough that clear isosbestic points could be obtained. Two sets of wavelengths on either side of the isosbestic points were selected and absorbance at these λ's were measured. The concentration of each species at a different pH was calculated from the following equation

$$C_1 = \frac{A(\lambda_1)\in_2(\lambda_2) - A(\lambda_2)\in_2(\lambda_1)}{\in_2(\lambda_1)\in_2(\lambda_2) - \in_1(\lambda_2)\in_2(\lambda_1)}$$

$$C_2 = C_T - C_1$$

where C_T is the total concentration of the compound in both forms and $\in_1(\lambda_1)$, $\in_1(\lambda_2)$, $\in_2(\lambda_1)$ and $\in_2(\lambda_2)$ are the molar extinction coefficients of species 1 and 2 at wavelengths λ_1 and λ_2 respectively. The latter were determined from the absorbance at a pH $\geq$ pKa $\pm$ 2 where only one species is present. The pKa for the equilibrium

$$\Phi NH_3^+ \rightleftharpoons \Phi NH_2 + H^+ \quad \Phi NH_3^+(\text{Monocation}) - \text{species 1}$$
$$\Phi NH_2(\text{Neutral}) - \text{species 2}$$

was calculated by using the equation

$$pKa = pH + \log \frac{C_1}{C_2}$$

Calculation of excited state acidity constant

The excited state acidity constants (p*K*a*) were obtained by using fluorimetric titration method (FT) [35]. In this method, the sample is excited at the isosbestic point and the intensities of monocation and neutral species are determined at their analytical wavelength under different pH conditions. A plot of (I/I_0) Vs pH for each species will give a sigmoid curve. pH at the meeting point of sigmoid curves will be the excited state p*K*a value.

Job's continuous variation method

Equimolar solutions of the 5AIQ and the β-CDx were prepared and mixed to standard volumes and proportions in order that the total concentration remained constant ($[5AIQ]_t + [\beta\text{-CDx}]_t = M$) but the ratio of the initial concentrations varied between 0 and 1. ΔOD values in the solutions of guests were calculated by measuring the absorbance of guest in the absence (A_0) and the presence (A) of β-CDx at each concentrations. Also, an equimolar solution of β-CDx was used as a blank, to take into account of refractive index.

Preparation of solid complexes

The solid 5AIQ-β-CDx complex was prepared using co-precipitation method. Physical mixture of 5AIQ and β-CDx was also prepared in order to serve as reference. 0.0585 g of 5AIQ was dissolved in 50 mL of methanol and the solution was added slowly to the saturated solution of β-CDx ($\approx$0.1243 g) in 50 mL water. The suspension formed, was stirred at 40°C for 30 min and stirring continued at room temperature for 24 h. The obtained mass was filtered through 0.45 μm membrane filter and dried at 40 °C in an oven for 24 h. The dried complex was ground to fine powder.

Results and discussion

Effect of acidity

The effect of acidity on the absorption spectra of 5AIQ has been studied in the range of pH 1.0–7.0 in absence and presence of β-CDx solutions. The absorption maxima of the neutral form of 5AIQ at pH 7.0 in aqueous and β-CDx solutions were at 329.8, 237.8 nm and 322.4, 234.8 nm, respectively. When pH was decreased, red shifted spectra were obtained around pH 3.5 for both the solutions. These spectra correspond to the monocation of 5AIQ obtained by the protonation of the amino group. The absorption maxima of monocation in aqueous and β-CDx solutions were 334.2, 258.4 nm and 333.2, 260.0 nm, respectively. The β-CDx solution is not stable and decomposes to glucose under high acidic conditions i.e., at below pH 1.0. As there was no change in absorption spectra when pH was decreased further up to 1.0, dication did not form in the pH range of 1.0–7.0.

On increase of pH from 7.0, no significant change was observed in the absorption spectra even up to pH 12.0. For monocation $\rightleftharpoons$ neutral equilibrium, clear isosbestic points at 348.2 and 348.6 nm were observed for aqueous and β-CDx solutions, respectively.

The fluorescence spectra of 5AIQ in aqueous solution at different pH values are shown in Fig. 1. The neutral species at pH 7.0 exhibits the fluorescence maximum at 455.0 nm. When pH is decreased, the maximum at 455.0 nm begins to disappear. The fluorescence intensity is quenched with the increase in acid concentration. At pH 1.5, a new spectrum begins to appear with the maximum around 431.0 nm. This spectrum may be due to the formation of monocation.

The fluorescence emission spectra of 5AIQ with 0.012 M β-CDx at various pH values are shown in Fig. 2. The neutral species appeared at pH 7.0 with the maximum at 444.0 nm. The fluorescence intensity decreases at 444.0 nm with the increasing acidity in the aqueous β-CDx solution. At pH 1.5,

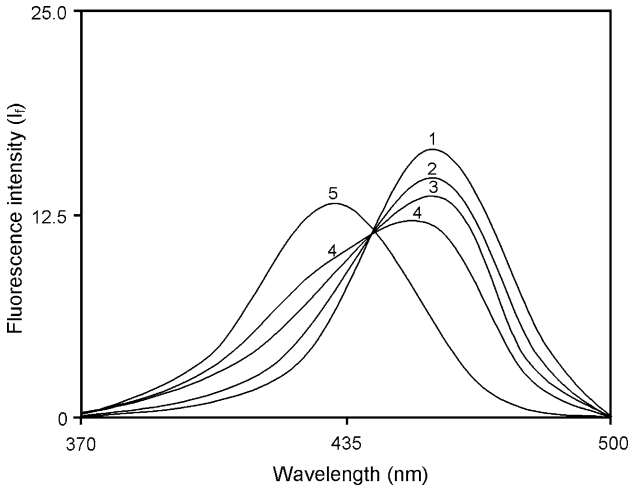

Fig. 1 Fluorescence spectra of 5AIQ (concentration = 2.30×10^{-5} mol dm^{-}) in the absence of β-CDx at different pH values: 1—pH 5.2, 2—pH 3.8, 3—pH 3.0, 4—pH 2.1, 5—pH 1.4 (λ_{exc} = 350.0 nm)

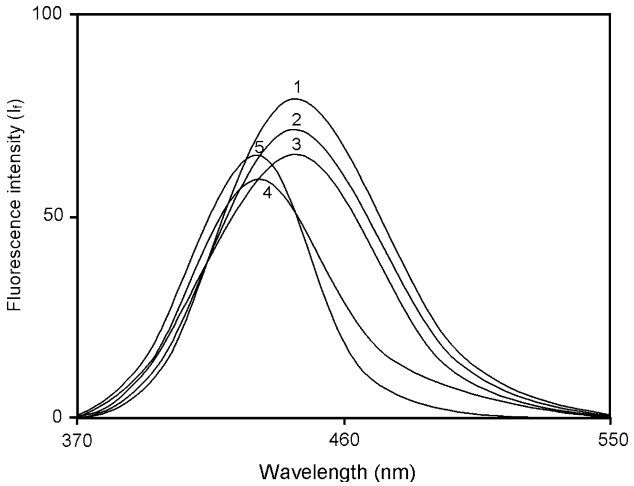

Fig. 2 Fluorescence spectra of 5AIQ (concentration = 2.30×10^{-5}M) with β-CDx at different pH values: 1—pH 5.8, 2—pH 4.3, 3—pH 3.5, 4—pH 2.8, 5—pH 1.4 ($\lambda_{exc} = 350.0$ nm)

a new fluorescence maximum appears at 435.0 nm. The blue shifted maximum is due to the formation of monocation obtained by the protonation of amino group in aqueous β-CDx medium. The absorption and emission spectral maxima of 5AIQ and its protonated form in aqueous and β-CDx media are given in Table 1.

Acidity constants

The ground and excited state acidity constant (p*K*a and p*K*a*) values for the equilibrium between neutral and monocation of 5AIQ in aqueous and β-CDx media were determined spectrophotometrically and by fluorimetric titration curves (FT curves) method. The ground and excited state acidity constant values of 5AIQ in aqueous and β-CDx media are given in Table 2. The p*K*a (see Table 2) values for neutral $\rightleftharpoons$ monocation equilibrium of 5AIQ in β-CDx medium is the same as in aqueous medium.

The plots of fluorescence intensities of 5AIQ at different pH values in aqueous and 1.2×10^{-2} M β-CDx for the above mentioned equilibria are given in Fig. 3. In aqueous medium, the FT curves for the equilibrium between monocation and neutral of 5AIQ (see Fig. 3a) meet at pH 3.1. The decrease of the neutral fluorescence intensity exactly corresponds to the increase of monocation fluorescence intensity and this reveals the absence of other processes such as proton induced fluorescence quenching. The middle of their inflection is taken as the excited state acidity constant (p*K*a*) value for the equilibrium between monocation and neutral form of 5AIQ in aqueous medium and it is 3.1.

The FT curves of monocation and neutral form of 5AIQ in β-CDx medium are drawn using the fluorescence intensities at 402.0 and 450.0 nm (see Fig. 3b). In this case also the fluorescence intensity decrease for neutral form of 5AIQ exactly corresponds to the increase of fluorescence intensity for the monocationic form. Therefore the excited state acidity constant value for the equilibrium between monocation and neutral is obtained from the mid point of these two curves to be 3.0. The equilibrium between monocation-neutral form of 5AIQ in β-CDx medium is very close to that in aqueous medium. There is no significant change in the p*K*a and p*K*a* values of 5AIQ in aqueous and β-CDx medium and this indicate that the amino group is not affected during the formation of inclusion complex between 5AIQ and β-CDx.

Inclusion complexation in aqueous medium

Absorption spectral studies

The absorption maxima, absorbance and fluorescence maxima of 5-aminoisoquinoline (5AIQ) at different concentrations of β-CDx at pH $\sim$6.8 are given in Table 3. At pH 6.8, 5AIQ exists as neutral form. Upon increasing the concentrations of β-CDx the absorption maxima are blue shifted with a gradual increase in the molar absorption coefficients for neutral form. The absorbance of the neutral form increases with the increase in β-CDx concentration up to 1.2×10^{-2} M at pH 6.8. At concentrations higher than 1.2×10^{-2} M the absorption maxima and absorbance remain unchanged. It reveals the completion of complex formation at 1.2×10^{-2} M concentration of β-CDx. The blue shift and increase in absorbance observed during the addition of β-CDx suggest the formation of inclusion complex between 5AIQ and β-CDx.

Figure 4 gives the plot of $1/\Delta A$ versus $1/[\beta\text{-CDx}]$ for the neutral form of 5AIQ. The linearity of the plot confirms the formation of 1:1 complex for neutral form of 5AIQ with β-CDx. From the slope of the straight line, the binding

Table 1 The absorption and emission spectral maxima of 5AIQ in the absence and presence of β-CDx at different pH

pH	Absorption maxima, nm						Fluorescence maxima, nm	
	Aqueous medium			β-CDx medium			Aqueous medium	β-CDx medium
5.0	329.8	237.8	–	322.4	234.8	–	455.0	444.0
1.5	334.2	258.4	225.2	333.2	260.0	–	431.0	435.0

Table 2 The ground and excited state acidity constant values of 5AIQ in aqueous and β-CDx media

Equilibrium	Acidity constants			
	Aqueous medium		β-CDx medium	
	p*K*a	p*K*a*	p*K*a	p*K*a*
Neutral ⇌ Monocation	3.2	3.1	3.2	3.0

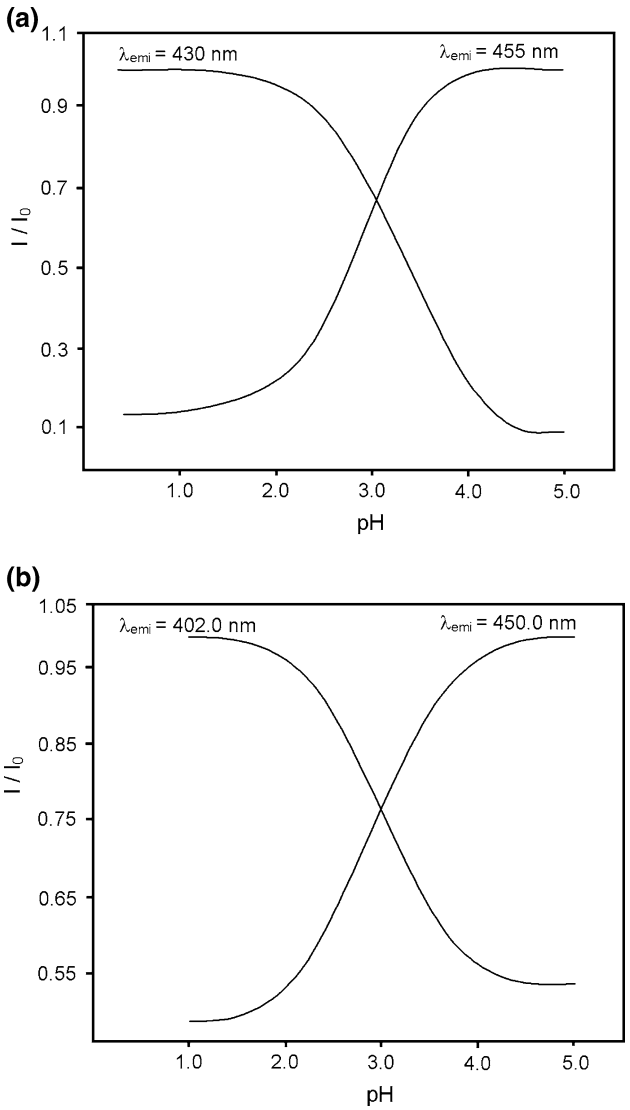

Fig. 3 Fluorimetric titration curves of 5AIQ in the absence of β-CDx (**a**) and in β-CDx (**b**)

constant 'K' was calculated to be 82.39 M^{-1} ($r = 0.998$, standard deviation = 0.0013) for the neutral form of 5AIQ at 303 K.

Steady state fluorescence spectral studies

The fluorescence spectrum of 5AIQ is more sensitive than the absorption spectrum when β-CDx is added to aqueous solution. Figure 5 shows the fluorescence emission spectra of 5AIQ at pH 6.8 with different concentrations of β-CDx. It is observed that the fluorescence intensity increases while increasing the concentrations of β-CDx at pH 6.8. This may be due to the encapsulation of the fluorophores in the relatively non-polar β-CDx cavity. Environment is changed for the guest molecules from the polar bulk water to the non-polar β-CDx cavity. An increase in the fluorescence intensity and red shift in fluorescence maxima of guest molecule while increasing concentrations of β-CDx during the formation of an inclusion complex have been reported earlier [36, 37].

Table 3 Absorption and fluorescence maxima of 5AIQ with different concentrations of β-CDx at pH 6.8

Concentrations of β-CDx, M	pH 6.8		
	λ_{max}, nm (abs)	λ_{max}, nm (abs)	λ_{flu}, nm
0	329.8 (0.148)	237.8 (0.518)	455
0.002	328.0 (0.177)	237.2 (0.588)	451
0.004	327.8 (0.198)	236.8 (0.653)	450
0.006	326.8 (0.229)	236.0 (0.729)	445
0.008	326.2 (0.260)	236.0 (0.809)	448
0.010	324.2 (0.282)	234.8 (0.886)	449
0.012	322.4 (0.307)	234.8 (0.943)	444

There is no increase in the fluorescence intensity of 5AIQ by the further addition of β-CDx. This shows the completion of complex formation at 1.2×10^{-2} M concentration of β-CDx for the neutral form of 5AIQ.

The plot of $1/(I - I_0)$ versus $1/[\beta - CDx]$ at pH 6.8 is given in inset Fig. 5 for neutral form of 5AIQ with β-CDx. The linearity of the plot reveals the formation of 1:1 complex between 5AIQ and β-CDx. From the slope and intercept of the straight line, the binding constant '*K*' was calculated to be 88.66 M^{-1} ($r = 0.991$, standard deviation = 1.214) at pH 6.8.

Time-resolved fluorescence spectral studies

The complexation between β-CDx and 5AIQ has also been investigated by the time resolved fluorescence technique. The fluorescence decay profiles were fitted to the expression.

$$I(t) = \sum_{i=1}^{n} \beta_1 \exp -(t/t_1) \quad (3)$$

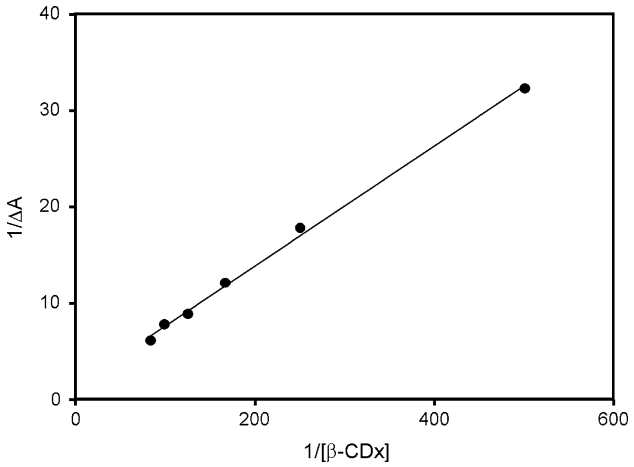

Fig. 4 Benesi–Hildebrand absorption plot for the 1:1 complex between 5AIQ (concentration = 2.30 × 10^{-5}M) and β-CDx at pH 6.8 (λ_{abs} = 325.0 nm)

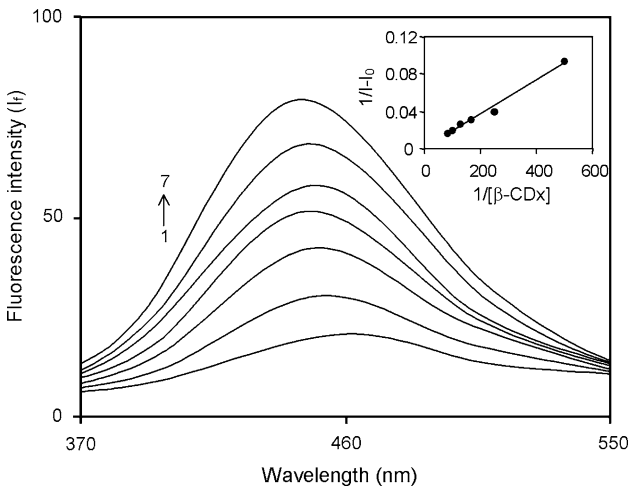

Fig. 5 Fluorescence spectra of 5AIQ (concentration = 2.30 × 10^{-5} mol dm^{-}) with different concentrations of β-CDx (1. 0, 2. 0.002, 3. 0.004, 4. 0.006, 5. 0.008, 6. 0.010 and 7. 0.012 M β-CDx) [Inset : Benesi-Hildebrand emission plot for the 1:1 complex between 5AIQ and β-CDx at pH 6.8 (λ_{emi} = 450.0 nm)]

where I(t) is the intensity of the fluorescence at time t, β is the pre-experimental factor for the fraction of the fluorescence intensity, t_1 is the fluorescence lifetime of the emitting species and n is the total number of emitting species.

In aqueous solution, the fluorescence decay of 5AIQ obtained from monitoring the emission at 450.0 nm is a single exponential with lifetime value of 2.51 × 10^{-9} ns (t_1). However in the presence of various concentrations of β-CDx, the fluorescence decay are fitted to double-exponential with the lifetimes of t_1 in the range of 2.46 × 10^{-9} to 2.17 × 10^{-9} ns and t_2 in the range of 6.35 × 10^{-9} to 8.08 × 10^{-9} ns (Table 4). The life-time of 6.35 × 10^{-9} to 8.08 × 10^{-9} ns and relative amplitudes of 5AIQ with increasing concentrations of β-CDx reveal the presence of another species which must be an inclusion complex of 5AIQ with β-CDx.

The ratio of the pre-exponential factors (B_2/B_1) is related to the concentration of the two components by the equation [38].

$$\frac{B_2}{B_1} = C_2 kr_2 \varepsilon_2 / C_1 kr_1 \varepsilon_1 \quad (4)$$

where, C, kr and ε are the concentration of 5AIQ, the radiative rate constant and the molar absorption co-efficient at the excitation wavelength respectively. The subscripts 1 and 2 refer the free and complexed form of 5AIQ, respectively. Since kr is a constant and $\varepsilon_1 = \varepsilon_2$, Eq. 5 is simplified as $B_2/B_1 \approx$ or $\propto C_2/C_1$. In excess of [β-CDx] with respect to the 5AIQ, B_2/B_1 can be written as Eq. 5.

$$\frac{B_2}{B_1} = K\ [\beta\text{-CDx}] \quad (5)$$

The plot of B_2/B_1 versus [β-CDx] is given in Fig. 6. The linearity of the plot also confirms the formation of 1:1 complex between 5AIQ and β-CDx. From the slope of the straight line, binding constant 'K' was calculated to be 87.89 M^{-1} which is nearly equal to the binding constant (88.66) calculated from fluorescence data.

Effect of glucose concentration with 5AIQ

In order to find out whether the spectral changes observed for 5AIQ are due to either inclusion complexation or hydrogen bonding interactions with hydroxyl group present in the β-CDx, the same set of experiments were carried out with varying concentrations of D(+)-glucose instead of β-CDx. There is no significant change in the absorption and fluorescence spectrum of 5AIQ with increasing the concentrations of D(+)-glucose. This shows that the enhancement in the fluorescence intensity and absorbance are not due to hydrogen bonding interaction with a glucose unit and further confirms the inclusion complexation of 5AIQ with β-CDx.

Job's method of analysis

The stoichiometry of the inclusion complex between 5AIQ and β-CDx was also confirmed by the plots of Job's continuous variation method using absorption and fluorescence data. The change in optical density (ΔOD) and fluorescence intensities (ΔI_f) were plotted against the mole fraction of 5AIQ, separately. In both plots ΔOD and ΔI_f are maximum at 0.5 indicating the stoichiometry of the complex is 1:1.

Table 4 Fluorescence lifetimes and the amplitudes of 5AIQ at pH 6.8 with and without β-CDx

Concentrations of β-CDx, M	Lifetime, s	Relative amplitude	χ^2	Standard deviation
0	2.35×10^{-9}	100	1.37	1.13×10^{-11}
0.002	2.10×10^{-9} 6.10×10^{-9}	45.32 54.68	1.33	2.69×10^{-11} 6.72×10^{-11}
0.004	2.05×10^{-9} 6.33×10^{-9}	38.71 61.29	1.32	3.62×10^{-11} 5.89×10^{-11}
0.006	1.99×10^{-9} 6.53×10^{-9}	30.79 69.21	1.17	4.23×10^{-11} 4.01×10^{-11}
0.008	1.82×10^{-9} 6.71×10^{-9}	28.01 71.99	1.22	4.23×10^{-11} 4.01×10^{-11}
0.010	1.75×10^{-9} 6.85×10^{-9}	20.53 74.47	1.15	5.80×10^{-11} 3.23×10^{-11}
0.012	1.54×10^{-9} 6.97×10^{-9}	15.31 84.69	1.26	6.30×10^{-11} 1.90×10^{-11}

Excitation wavelength = 350.0 nm, detection wavelength = 450.0 nm

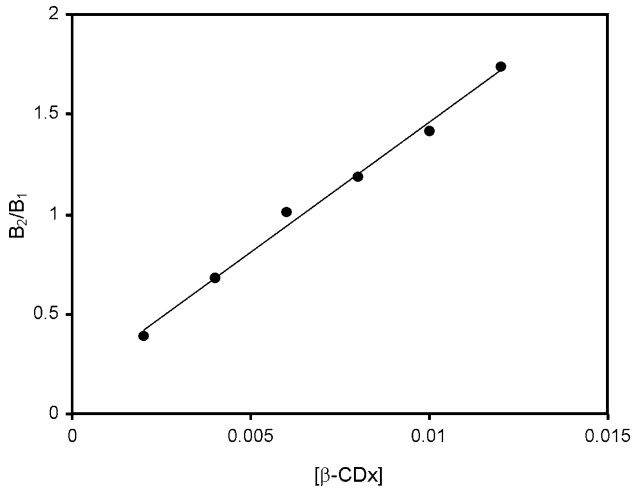

Fig. 6 Plot of B_2/B_1 versus [β-CDx]

Inclusion complexation in solid state

To confirm the formation of inclusion complex between 5AIQ and β-CDx, the solid complex was prepared by co-precipitation method and analysed by FT-IR spectral and microscopic morphological studies.

The FT-IR spectra of pure β-CDx, 5AIQ, physical mixture of 5AIQ with β-CDx and solid inclusion complex between 5AIQ and β-CDx were recorded and given in Fig. 7. The stretching frequencies of N–H, C–H (aromatic) and C = N appeared at 3310.04, 3175.38 and 1578.56 cm^{-1}, respectively in the pure 5AIQ (Fig 7b). These frequencies were also observed for physical mixture of 5AIQ and β-CDx (Fig 7c). But in the case of solid inclusion complex, the N–H and C–H (aromatic) stretching frequencies of 5AIQ disappeared i.e., they are merged with the stretching frequencies of primary and secondary O–H groups of β-CDx and appeared at 3370.15 cm^{-1}. Further the C=N stretching frequency also significantly changed to 1637.59 cm^{-1} in the solid complex (Fig 7d). No change was observed in the frequencies of N–H, C–H and C=N for the physical mixture between 5AIQ and β-CDx. These changes in FT-IR spectra

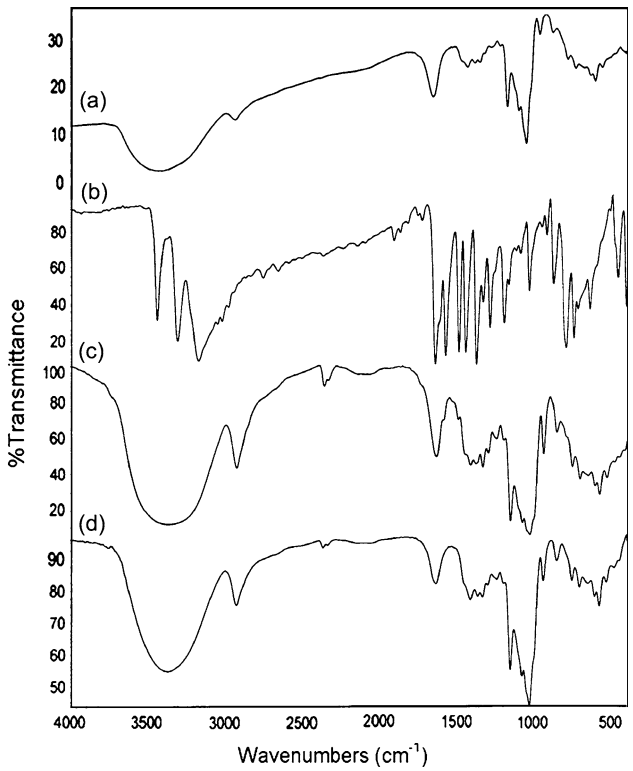

Fig. 7 FT-IR spectra of **a** pure β-CDx, **b** pure 5AIQ, **c** physical mixture of 5AIQ with β-CDx, and **d** solid inclusion complex of 5AIQ with β-CDx

indicate the formation of inclusion complex between 5AIQ and β-CDx in solid state.

Supporting evidence for complexation of 5AIQ with β-CDx was also obtained from analysis of the SEM images. SEM pictures were taken at two different magnifications (×500 and ×2000) for β-CDx, 5AIQ, physical mixtures of 5AIQ: β-CDx and inclusion complex (Fig. 8) SEM images of inclusion complex (Fig. 8g, h) show a compact and homogeneous powder-like structure. They are different from the images of β-CDx (Fig. 8a, b), 5AIQ (Fig. 8c, d) and the physical mixture of 5AIQ with β-CDx. Structure of β-CDx is clearly shown from the SEM images physical mixtures (Fig. 8e, f).

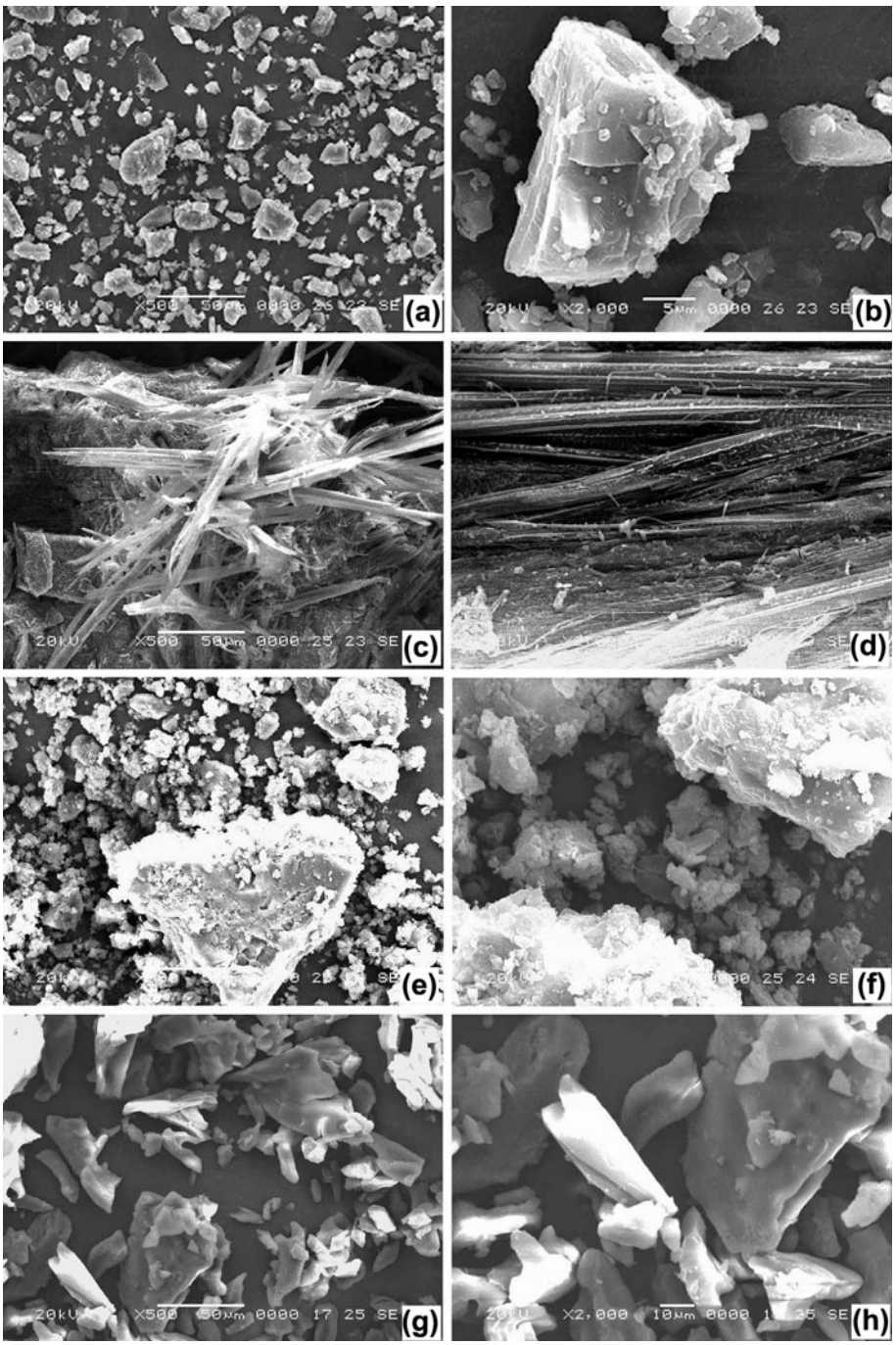

Fig. 8 SEM images of **a** pure β-CDx (×500), **b** pure β-CDx (×2000), **c** pure 5AIQ (×500), **d** pure 5AIQ (×2000), **e** physical mixture of 5AIQ with β-CDx (×500), **f** physical mixture of 5AIQ with β-CDx (×2000), **g** solid inclusion complex of 5AIQ with β-CDx (×500) and **h** solid inclusion complex of 5AIQ with β-CDx (×2000)

FT-IR spectral study and SEM image analysis confirm the formation of inclusion complex between 5AIQ and β-CDx

Calculations using the software MOPAC/AM1 show that the lengths of 5AIQ molecule and its monocation $5AIQH^+$ are 7.66 and 7.71 Å, respectively (Table 5). The length of β-CDx is 7.8 Å. Hence, there is a possibility for complete accommodation of whole molecule within the cavity of β-CDx. But the low values of binding constant (K) revealed partial accommodation of whole molecule in β-CDx cavity. Here K is an important parameter to characterize the inclusion interaction of guest with β-CDx and also reflects the intensity of binding forces of β-CDx with guest molecule. Absence of a change in p*K*a value during complexation reveals the presence of NH_2 group outside the β-CDx cavity. This also confirms the partial accommodation of 5AIQ. Based on these results, the structures of inclusion

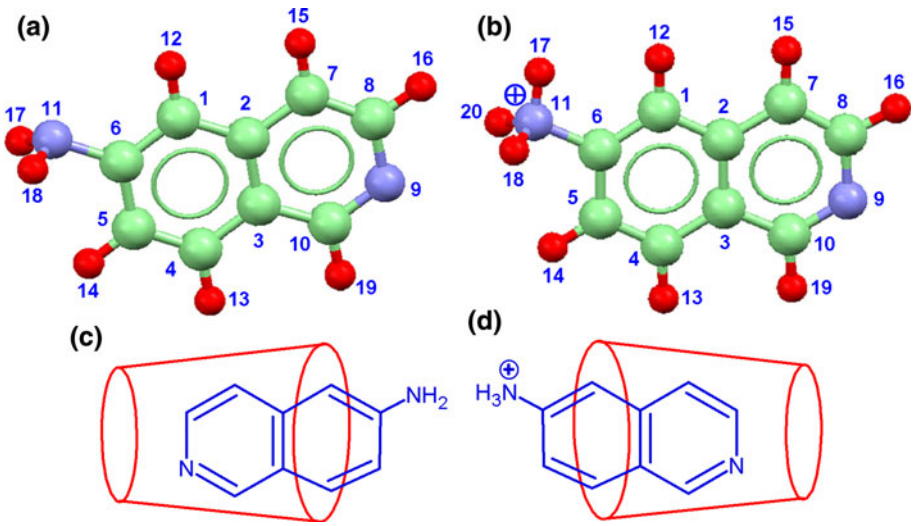

Fig. 9 MOPAC/AM1 of **a** optimized structure of 5AIQ, **b** optimized structure of $5AIQH^{\oplus}$, **c** schematic diagram of inclusion complex (1:1) of 5AIQ with β-CDx and **d** schematic diagram of inclusion complex (1:1) of $5AIQH^{\oplus}$ with β-CDx

Table 5 Bond lengths between various atoms of 5AIQ and its monocation

Atoms	Bond distance (Å)
Neutral	
H_{16}–H_{18}	7.66
C_8–H_{17}	6.68
N_9–H_{14}	5.83
H_{12}–H_{13}	5.02
Cation	
H_{16}–H_{18}	7.71
H_{16}–H_{20}	7.10
C_8–H_{17}	6.72
C_8–H_{20}	6.24
N_9–C_5	4.86
H_{12}–H_{13}	5.03

complexes of 5AIQ and its monocation in β-CDx are proposed as in Fig. 9 [39].

Conclusions

The effects of β-CDx on the neutral form of 5AIQ have been investigated by absorption and fluorimetric techniques. The stoichiometry of 5AIQ with β-CDx complex, determined by Benesi-Hildebrand equation and Job's continues variation method is 1:1. The binding constant values calculated by different methods are found to be nearly equal. The formation of inclusion complex between 5AIQ and β-CDx has also been confirmed by the Time-resolved fluorescence spectral study in aqueous solution and by FT-IR spectral study and microscopic morphological image analysis in solid state. The acidity constant values determined by absorption and fluorescences data of 5AIQ for the equilibrium between neutral and monocation in aqueous medium are nearly same as the values in β-CDx medium. As there is no change in the p*K*a and p*K*a* values of 5AIQ in aqueous and β-CDx media, we can conclude that the protonation of amino group is not affected by the complexation between 5AIQ and β-CDx. Based on the above results the structure of 1:1 inclusion complex between 5AIQ and β-CDx has been proposed.

Acknowledgement We are grateful to the National Centre for Ultrafast Processes, University of Madras, Chennai, for the assistance in the measurements of the fluorescence lifetimes.

References

1. Saenger, W.: Angew. Chem. Int. Ed. Engl. **19**, 344 (1980)
2. Bender, M.L., Komiyama, M.: Cyclodextrin Chemistry. New York, Springer (1978)
3. Uekama, K., Hirayama, F.: In: Wermuth, C.G. (ed.) The Practice of Medicinal Chemistry, p. 793. Academic Press, London (1996)
5. Tabushi, I.: Cyclodextrin catalysis as a model for enzyme action. Acc. Chem. Res. **15**, 66–72 (1982)
6. Tabushi, I., Kuroda, Y.: Cyclodextrins and cyclophanes as enzyme models. Adv. Catal. **32**, 417–466 (1983)
7. Szejtli, J.: Cyclodextrin and Their Inclusion Complexes. Academic Kiado, Budapest (1982)
8. Szejtli, J.: Cyclodextrin Technology. Kluwer, Dordrecht (1988)
9. Ramamurthy, V., Weiss, R.G., Hammond, G.: Adv. Photochem. **18**, 67 (1993)
10. Kalyanasundaram, K.: Photochemistry in Microheterogeneous Systems. Academic Press, New York (1987)
11. Bortolus, P., Monti, S.: Adv. Photochem. **21**, 1 (1996)
12. Kleinman, M.H., Bohne, C.: Organic Photochemistry: Molecular and Supramolecular Photochemistry, p. 838. Marcel Dekker Inc, New York (1997)
13. Santra, S., Dogra, S.K.: Spectral characteristics of 2-(2′-aminophenyl) benzimidazole in b-cyclodextrin. J. Photochem. Photobiol. A: Chem. **101**, 221–227 (1996)
14. Burai, T.N., Panda, D., Datta, A.: Fluorescence enhancement of epicocconone in its complexes with cyclodextrins. Chem. Phys. Lett. **455**, 42–46 (2008)

15. Sainz-Rozas, P.R., Isai, J.R., Sanchez, M., Tardajos, G., Gonzelez-Gaitano, G.: Effects of natural cyclodextrins on the photophysical properties of dibenzofuron-2-carboxylic acid. J. Phys. Chem. A **108**, 392–402 (2004)
16. Armarego, W.L.F.: Fused Pyrimidines: Part I-Quinazolines. Interscience, New York (1967)
17. Kametani, T., Fukumoto, K.: Isoquinolines Part 1, vol. 38. John Wiley, New York (1981)
18. Fry, D.W., Kraker, A.J., McMichael, A., Ambroso, L.A., Nelson, J.M., Leopold, W.R., Connors, R.W., Bridges, A.J.: A specific inhibitor of the epidermal growth factor receptor tyrosine kinase. Science **265**, 1093–1095 (1994)
19. Traxler, T.M., Furet, P., Melt, H., Buchdunger, E., Meyer, T., Lydon, N.: 4-(Phenylamino)pyrrolopyrimidines: # potent and selective, ATP site directed inhibitors of the EGF-receptor protein tyrosine kinase. J. Med. Chem. **39**, 2285–2292 (1996)
20. Hynes, J.B., Tomazić, A., Kumar, A., Kumar, V., Freisheim, J.H.: Inhibition of human dihydrofolate reductase by 2,4-diaminoquinazolines bearing simple substituents on the aromatic ring. J. Heterocycl. Chem. **28**, 1981–1986 (1991)
21. Harris, N.V., Smith, C., Bowden, K.: Antifolate and antibacterial activities of 5-substituted 2, 4-diaminoquinazolines. J. Med. Chem. **33**, 433–444 (1990)
22. Dempcy, R.O., Skibo, E.B.: Rational design of quinazoline-based irreversible inhibitors of human erythrocyte purine nucleoside phosphorylase. Biochemistry **30**, 8480–8487 (1991)
23. Neumeyer, J.L., Weinhardt, K.K., Carrano, R.A., McCurdy, D.H.: Isoquinolines. 3. 3-Aminoisoquinoline derivatives with central nervous system depessant activity. J. Med. Chem. **16**, 808–813 (1973)
24. Shun-li, W., Tze-wei, Y., Tong-Ing, H.: Photophysics and excited-state proton transfer of 2′-hydroxy-2-trans-styrylquinoline. Chem. Phys. Lett. **418**, 397–401 (2006)
25. Dey, J.K., Dogra, S.K.: Dual fluorescence of 2-[4-(Dimethylamino)phenyl]benzothiazole and its benzimidazole analog: effect of solvent and pH on electronic spectra. J. Phys. Chem. **98**, 3638–3644 (1994)
26. Kothai Nayaki, S., Swaminathan, M.: A study of solvatochromism and proton transfer kinetics of 2, 2′-dihydroxybiphenyl. J. Photochem. Photobiol. A.: Chem. **102**, 217–221 (1997)
27. Kothai Nayaki, S., Swaminathan, M.: Unusual luminescence characteristics of aminobiphenyls. Spectrochim. Acta A **58**, 2931–2940 (2002)
28. Sivakumar, P., Kothai Nayaki, S., Swaminathan, M.: Photophysical behaviour of 2, 6-diaminoanthraquinone in different solvents and at various pH. Spectrochim Acta **68**, 651–655 (2007)
29. Enoch, I.M.V., Swaminathan, M.: Fluorimetric and prototropic studies on the inclusion complexation of 2-amino and 4-aminodiphenyl ethers with β-cyclodextrin: Unusual behavior of 4-aminodiphenyl ether. J. Lumin. **127**, 713–720 (2007)
30. Rajamohan, R., Kothai Nayaki, S., Swaminathan, M.: Inclusion complexation and photoprototropic behaviour of 3-amino-5-nitrobenzisothiazole with β-cyclodextrin. Spectrochim. Acta A **69**, 371–377 (2008)
31. Rajamohan, R., Kothai Nayaki, S., Swaminathan, M.: Spectrofluorimetric study on inclusion complexation of 2-amino-6-fluorobenzothiazole with β-cyclodextrin. Collect. Czech. Chem. Commun. **73**, 147–160 (2008)
32. Jorgenson, M.J., Hartter, D.A.: A critical re-evaluation of the hammett acidity function at moderate and high acid concentrations of sulfuric acid. New H_0 values based solely on a set of primary aniline indicators. J. Am. Chem. Soc. **85**, 878–883 (1963)
33. Benesi, H.A., Hildebrand, J.H.: A spectrophotometric investigation of the interaction of iodine with aromatic hydrocarbons. J. Am. Chem. Soc. **71**, 2703–2707 (1949)
34. Cho, D.W., Kim, Y.H., Yoon, M., Kang, S.G., Kim, D.: Cyclodextrin effects on intramolecular charge transfer of 2-biphenylcarboxylic acid: a pre-twisted molecule. J. Chem. Soc. Faraday Trans. **92**, 29–33 (1996)
35. Lasser, N., Feitelson, J.: Excited state pK values from fluorescence measurements. J. Phys. Chem. **70**, 1011–1016 (1973)
36. Hoshino, M., Imamura, M., Ikehara, K., Hamai, Y.: Fluorescence enhancement of benzene derivatives by forming inclusion complexes with beta.-cyclodextrin in aqueous solutions. J. Phys. Chem. **85**, 1820–1823 (1981)
37. Al-Hassan, K.A., Klein, V.K.A., Sawaiyan, A.: Normal and twisted intramolecular charge-transfer fluorescence of 4-dimethylaminobenzonitrile in α-cyclodextrine cavities. Chem. Phys. Lett. **212**, 581–587 (1993)
38. Monti, S., Kohler, G., Grabner, G.: Photophysics and photochemistry of methylated phenols in beta.-cyclodextrin inclusion complexes. J. Phys. Chem. **97**, 13011–13016 (1993)
39. Nayak, M.K., Dogra, S.K.: Photophysics of 1-hydroxy-9-fluorenone: absence of excited state intramolecular proton transfer reaction. J. Photochem. Photobiol. A **169**, 79–88 (2005)